

## HIGH-SPEED FABRICATION OF LASER DOPING SELECTIVE EMITTER SOLAR CELLS USING 532NM CONTINUOUS WAVE (CW) AND MODELOCKED QUASI-CW LASER SOURCES

J.M. Bovatsek<sup>\*1</sup>, A. Sugianto<sup>2</sup>, B. Hallam<sup>2</sup>, B. Tjahjono<sup>2,3</sup>, S. Wenham<sup>2</sup>, R.S. Patel<sup>1</sup>  
<sup>1</sup>Spectra Physics

3635 Peterson Way, Santa Clara, CA. 95054, USA

<sup>2</sup>ARC Centre of Excellence for Advanced Silicon Photovoltaics and Photonics,  
University of New South Wales, Sydney, NSW 2052, Australia

<sup>3</sup>Sunrise Global Solar Energy Co. Ltd.

No. 1, Sec. 2, Ligong 1st Rd., Wujie Township, Yilan Country 268, Taiwan

\*Tel: +14089805735, Fax: +14089873156, email: [jim.bovatsek@newport.com](mailto:jim.bovatsek@newport.com)

**ABSTRACT:** In recent years, laser doping of selective emitters (LDSE) has demonstrated great promise for improving c-Si solar cell performance with the potential for low cost of adaptation. Absolute cell efficiency improvement of 1 – 2 % is seen with a process pioneered at the University of New South Wales which couples narrow-line LDSE processing with a self-aligning, light-induced plating (LIP) metallization process. To help transfer this technology to the manufacturing floor, it is important to find and characterize the ideal laser source for LDSE processing. Current laser sources that may be considered include continuous wave (CW) and mode-locked (ML) quasi-CW laser sources. The output to these lasers make them well-suited for localized heating and melting of materials, and they can be built at various wavelengths, such as near infrared (NIR) at 1064 nm, green at 532 nm, and ultraviolet (UV) at 355 nm. While both CW and ML lasers might be good choices, they are vastly different in both their optical radiation output profile and their technological architectures. These differences could have important ramifications for manufacturability of LDSE solar cells. As such, we have in this work characterized both CW and modelocked laser technologies for LDSE processing. With optical emission at the 532-nm wavelength, LDSE features were created at scan speeds of 2 to 12 m/s and power levels from 12 – 15W. LIP metallization was used for final cell fabrication. Efficiencies of 17.4 – 18.4% and fill factors from 77 – 79% are typically achieved. LDSE cells fabricated with 355-nm ML laser source were also compared. Theoretical considerations with regard to the wavelength and laser type are explored; and the suitability of the various laser sources for large-scale production is discussed.

**KEYWORDS:** laser doping, selective emitters, silicon solar cells

### 1 INTRODUCTION

Fabrication of selective emitters suitable for c-Si solar cell production is an active area of research. By selectively doping specific regions of the wafer surface and applying a suitable metallization layer, researchers have clearly demonstrated that cell efficiency improvements can be generated. And yet, widespread adoption of the selective emitter architecture in the manufacturing environment has remained somewhat elusive.

Many different techniques for forming selective emitters have been demonstrated, each with varying degrees of complexity and resulting cell improvement. In one instance [1], researchers at the University of Stuttgart have used the residual phosphosilicate glass (PSG) from  $\text{POCl}_3$  furnace diffusion as the dopant source for a laser doping process. This approach is attractive to industry because it is minimally disruptive to the existing manufacturing process flow and is compatible with conventional screen print metallization.

Several more exotic methods have also shown varying degree of promise, involving for example, liquid chemical jet-guided laser beams (“LCP”) [2] and wet chemical etch-back selective emitter formation [3, 4]. More recently, a patterned direct ion implantation technique [5] has been shown to offer good cell performance with good potential for scale-up to high-volume manufacturing. A survey of the relevant literature indicates these methods generally result in cell efficiency gains of ~0.4 – 0.6% over standard screen-printed cells.

In this work, we focus on a method combining direct

laser-patterning of the selective emitter with a self-aligning metallization process, commonly referred to as the laser doped selective emitter (LDSE). This approach has been patented and pioneered by researchers at the ARC Photovoltaics Centre for Excellence at the University of New South Wales in Sydney, Australia [6, 7]. While various traditional laser sources have been tested for this process, here we explore the potential benefit of more novel laser technologies for high-speed LDSE fabrication.

#### 1.1 Basic phenomena in LDSE processing

LDSE processing involves irradiating a dopant-coated wafer surface with a focused laser beam, resulting in heating and melting of silicon, and the diffusion therein of phosphorus ions. This locally and heavily doped *selective emitter* is patterned in the geometry desired for the front contact finger lines and busbars, which are formed via a self-aligning light-induced plating (LIP) metallization process according to Durkee [8].

The majority of the processing for the LDSE solar cells are the same as is used for conventional screen printed solar cells, up to the end of the screen print/firing of the Aluminum rear. After this, the laser doping and LIP steps are performed. For the laser doping step, the wafer is spin- or spray-coated with a phosphoric acid ( $\text{H}_3\text{PO}_4$ ) solution. The resulting spin/spray-on doping (SOD) layer should be coated as uniformly as possible across the wafer.

A high-power laser beam is then focused onto the wafer surface and scanned at high speed – up to several meters per second. During the laser irradiation time, there

is sufficient heat deposited under the focused beam to cause melting of the silicon, removal of the ARC layer, vaporization of the  $\text{H}_3\text{PO}_4$  solution, and finally, diffusion of phosphorous ions into the silicon, thus forming a localized, heavily-doped  $n^{++}$  emitter region. After rinsing the residual SOD, the LDSE-patterned wafer is ready for LIP metallization. This general process is illustrated schematically in Figure 1.

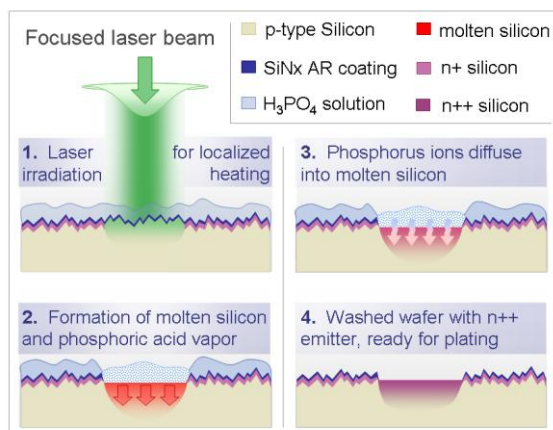


**Figure 1:** Illustration of basic physical phenomena involved in LDSE processing

In this work, the above-described LDSE procedure was executed using a variety laser sources and process parameter sets.

## 2 LASER TECHNOLOGY FOR LDSE

In recent years, many different lasers have been tested for fabrication of various laser-assisted selective emitter solar cells. One particular type—the 532-nm CW laser—has in fact very recently shown great promise in a high-volume production line environment [9]. In this paper, we explore various alternative laser sources in comparison to the 532-nm CW laser.

### 2.1 Wavelength considerations for LDSE

One of the most important parameters governing laser-material interactions is the optical wavelength, which generally defines the strength of the coupling of the laser energy to the material of interest. This “coupling” is generally characterized by the absorption depth, characterizing the extent to which the incident light is initially distributed within the bulk of the material. Greater penetration depths will generally result in rapid heating of a large volume of material, whereas shallower penetration will more efficiently melt a thinner layer of material.

For industrial processing with diode-pumped solid state (DPSS) lasers, the dominant wavelengths are those generated with neodymium-doped media coupled with various harmonic conversion optics—namely 1064 nm (fundamental laser emission line), 532 nm (2<sup>nd</sup> harmonic), 355 nm (3<sup>rd</sup> harmonic), etc.

Different materials absorb these wavelengths to different degrees. For optically transparent materials (glasses, crystals, etc.), one generally needs to go to the ultraviolet end of the spectrum (355-nm, or even 266-nm) to achieve good coupling of laser light to the material. Conversely, for the case of many metals, all optical

wavelengths—even those in the infrared domain (i.e. 1064 nm)—are absorbed nearly equally well. For semiconductor materials, such as silicon, the picture is not so straightforward.

Silicon has a bandgap energy of  $\sim 1.12$  eV, corresponding to an optical wavelength of  $\sim 1.11$   $\mu\text{m}$ . Above this wavelength, light is easily passed through the material. For shorter wavelengths, the light is absorbed—but to varying degrees and for a fairly wide range of wavelengths of interest.

For infrared 1064-nm light, there is significant penetration of the light to a depth of about 100  $\mu\text{m}$  into the silicon [10]. This is somewhat large in the context of LDSE processing, where the targeted junction depths are much closer to 1  $\mu\text{m}$ . With such a deep optical penetration depth, the 1064-nm light would seem a crude tool for laser doping; and researchers have indeed shown that unwanted damage to the silicon occurs alongside the doping process [11]

At the other extreme of common wavelengths is 355 nm, with optical penetration in silicon of only about 10 nm. This shallow depth of energy distribution implies that an optically-efficient process could result, with a relatively low laser intensity needed to form a thin melt layer in the silicon. However, for deeper melt regions of 1 to several micrometers, a 355-nm based process would require additional thermal diffusion to augment the shallow optical penetration depth. The net effect of this would be to require a longer dwell time of the laser beam on a given area of the material, which is had at the expense of processing speed.

In between these extremes is the 532-nm wavelength—irradiating the silicon to a depth of  $\sim 1$   $\mu\text{m}$ —matching quite well with desired junction depths. This relatively close match should result in an intrinsically-efficient process, with the near-instantaneous 1- $\mu\text{m}$  irradiation depth providing a good “launch pad” from which the (slower) thermal diffusion process can take over. In theory, with the assumption that sufficient laser power can be continuously applied to the silicon, there is no limit on the processing speed that can generate junction depths of  $\sim 1$   $\mu\text{m}$  with 532-nm irradiation. Based on these optical absorption considerations, 532-nm and 355-nm were chosen to study for LDSE fabrication.

### 2.2 Continuous wave vs. modelocked laser output

Besides wavelength, the temporal distribution of the laser output is another intrinsic laser parameter that is of significant interest. Laser temporal emission can range from continuous wave (CW)—having no significant power variation on the relevant timescales—to pulsed output of just 10’s or 100’s of pulses per second.

Intuitively, it would seem that having a constant source of heat that can be focused and scanned across the wafer would be an ideal tool for LDSE processing. In fact, such a source (15-W, 532-nm Spectra Physics *Millennia Prime* laser) has demonstrated good LDSE processing, and is one of the lasers chosen for these [11].

ML lasers are a possible alternative type of laser for LDSE. ML lasers operate with a pulse repetition frequency of 10’s of MHz –  $\sim 80$  MHz in our study. At such a high PRF, these lasers can almost be considered as CW; hence they are sometimes referred to as quasi-CW (QCW) lasers. Another common aspect of ML lasers is that the output pulse durations are typically very short—on the order of 10’s of picoseconds. A schematic representation of CW vs. ML laser output intensity vs.

time is shown in Figure 2, for the case of 10-W of average power.

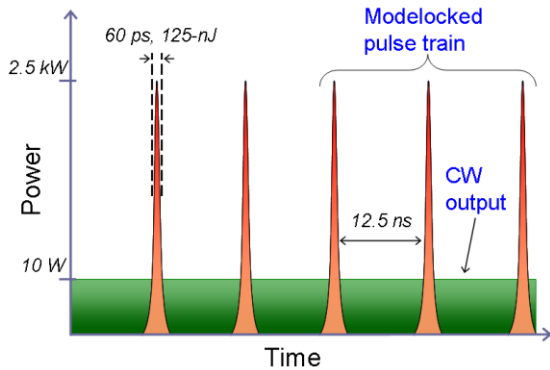


**Figure 2:** Laser emission with time of 10-W average power ML and CW lasers.

With the laser’s power output confined to a 60-ps pulse at 12.5-ns intervals, the 10-W average power output of the ML laser translates to a substantially higher *peak power* of 2.5 kW, as defined by the pulse energy divided by the pulse duration. And combined with the very short time between these pulses, it seems plausible that this pulsed output could rapidly heat and melt the silicon, possibly with higher efficiency compared to CW irradiation.

Thus, while the 532-nm CW laser source has demonstrated good performance for LDSE processing, there appears to be the possibility of improved performance with alternative laser technologies. With the shallow absorption of the 355-nm UV wavelength, there may be an accompanying process efficiency gain through lower power requirements. Likewise, with the high-PRF and high-peak power of modelocked laser pulses, the case can also be made for potentially higher-speed processing. With these considerations, we have chosen two modelocked laser sources, operating at the 355-nm and 532-nm wavelengths, to compare to the 532-nm *Millennia Prime* CW source for LDSE solar cell fabrication.

### 3 EXPERIMENT PROCEDURES

Two separate studies were conducted. In one study, LDSE cell performance for a 532-nm CW laser process was compared to that of a 355-nm ML laser; and a follow-up study comparing the same 532-nm CW laser to a 532-nm ML source. Both ML sources are based on the same architecture, and hence have similar pulse durations (~60 ps) and pulse repetition frequencies (80 MHz). Besides the wavelengths, the other primary difference was the available output power: 12 W at 355-nm and >15 W for 532-nm output.

While both groups of wafers used for the two studies were p-type CZ single crystal <100> silicon, the processing of the wafers prior to laser doping was not identical. The primary differences were the type of surface texturing and the constitution of the ARC layer. Accordingly, the results of the two studies are not necessarily cross-comparable with each other. The size of the finished cells tested in the studies was in the range 4 – 7 cm<sup>2</sup>.

#### 3.1 General LDSE Fabrication Process

The wafer samples used in this work consisted of alkali textured p-type Cz silicon wafers. The wafers are then phosphorous diffused, and the SiNx ARC applied. After aluminum screen printing for back side metallization, these samples were then spin-coated with H<sub>3</sub>PO<sub>4</sub>. Typical spin parameters to achieve a good, uniform coating are 30 seconds at 3500 RPM. Immediately after spin coating, the laser-doping step was executed, followed by a rinse-off of the residual H<sub>3</sub>PO<sub>4</sub>. Finally, front-side contacts were formed via LIP metallization technique.

#### 3.2 Laser processing

For each of the studies performed, the laser processing procedures were more or less identical. After application of the SOD to the wafers, a 2-axis scanning galvanometer system (*Scanlab hurrySCAN II*) coupled with an f-theta focusing objective (~250-mm focal length) scanned the laser beam across the wafers in the desired metallization pattern (single-bus bar design, 1-mm finger line spacing). For all lasers used in both studies, the focused beam diameter at the wafer surface was approximately 18-20 μm (at 1/e<sup>2</sup> of peak intensity).

Two critical parameters in LDSE processing are laser power and scan speed. The scan speed is of particular interest because it directly impacts the LDSE production throughput that can be achieved. Laser powers tested were in the range of 8 – 15 W, and scan speeds were on the order of several meters per second. Table I below summarizes the parameters used for the two studies.

**Table I:** Summary of parameters used in the two studies

Study	Laser type	Wavelength (nm)	Output Power (W)	Scan speed (m/s)
1	CW	532	12	2, 6
1	ML	355	12	2, 6
2	CW	532	12	2, 4
2	CW	532	15	4, 8
2	ML	532	12	4, 8
2	ML	532	15	8, 12

For the first study, the parameters between the two lasers were chosen to be identical, since the primary intent was to characterize cell performance for identical process conditions. In addition, while the *Millennia* 532-nm CW laser is capable of 15-W power output, only 12 W was used for the study, as this is the limit of the 355-nm ML laser.

In the second study, the parameter set is more extensive, with two different power levels and a wider range of speeds tested for each laser. Also, note that higher speeds were tested with the modelocked laser system; this is due to preliminary findings which indicated that, at the same power level, the ML laser could melt the silicon with higher scan speeds compared to the CW laser.

#### 3.3 Light induced plating metallization

Immediately following laser-scanning of the metallization pattern on the wafers, the residual phosphoric acid is rinsed off with de-ionized water. Then,

after a 30-second 1% HF deglazing bath, light-induced plating (LIP) metallization was performed. Initially, a thin nickel seed layer is formed, which is followed by the primary copper deposition. Both steps were performed using the LIP method.

### 3.4 Analysis techniques

After the wafers were processed, IV data was generated using [insert hardware, methods, etc. provided by UNSW]. While this data is the primary determinant of success for any LDSE process, there are other analytical techniques that can be used to characterize the laser doping features themselves. To characterize the width and strength of the laser-melted region, as well as the extent of ARC removal, a metallurgical optical microscope is used. However, this tells nothing about the melt depth (and therefore doping/junction depth). To acquire this information, the standard technique is secondary ion mass spectrometry (SIMS) analysis. SIMS analysis for select features was performed in this study. Also, an alternative technique for characterizing junction depth was employed, involving angle-lapping and junction-staining of the wafer cross-section, followed by inspection with optical microscope.

## 4 RESULTS

### 4.1 First study: 532-nm CW vs. 355-nm ML

IV data were generated for two cells of each process parameter for both laser systems. The average of the data points are compiled in bar chart format and displayed in Figure 3 below.

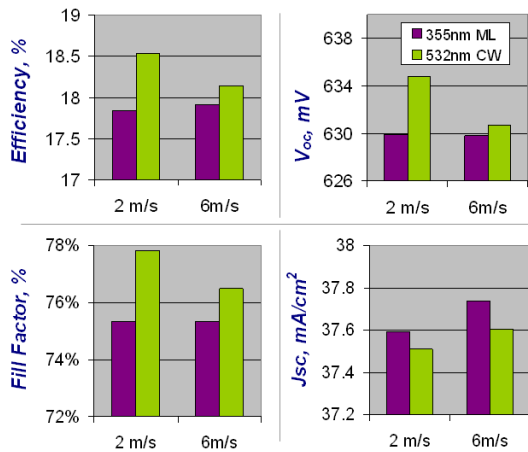


**Figure 3:** IV data for LDSE solar cells fabricated with 532-nm CW and 355-nm ML lasers at 2- & 6-m/s.

By nearly all metrics, the 532-nm CW LDSE cells were found to be superior to those fabricated with the UV ML laser. In terms of overall cell efficiency  $\eta$ , the CW laser source generated  $>18.5\%$  for the low speed

condition, whereas the 355-nm ML laser did not reach the 18% mark for any condition. Even for the higher speed of 6 m/s, the CW cells were better performing than those fabricated at the lower 2-m/s speed with the 355nm ML laser.

### 4.2 Second study: 532-nm CW vs. 532-nm ML

The second study created a much larger data set, with a significantly wider range of process conditions tested. Considering that the scan speed for good LDSE fabrication changes with different power levels, it is logical to compare the best speed for each of the two power levels tested. Such a comparison is displayed in Figure 4, which shows best-cell performance at the 12 & 15W power levels for the two laser systems. For the ML-processed cells, the scan speeds for the 12- and 15-W power levels were 8- and 12-m/s, respectively; for the CW cells, the corresponding speeds were 4- and 8-m/s (50% and 33% lower, respectively).

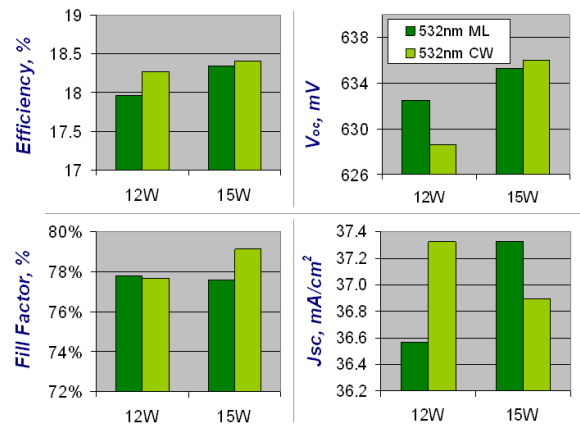


**Figure 4:** Best-speed/best-cell performance for 12- & 15-W CW & ML laser power.

The data displayed in Figure 4 illustrate that CW-laser processing resulted in higher performing cells. At the same time, however, the speed at which these cells were fabricated is significantly less than that for the ML laser at the same power level. For both lasers, there is a fairly consistent trend of better cell performance with increased laser power, which is also achieved at high scan speeds.

### 4.3 Best-cell data

To summarize the cell performance results of the two studies, Table 3 below shows best-cell performance for each laser within the respective study.

**Table 3:** Best cell performance of each laser in each study.

Test	Laser type	Speed (m/s)	V <sub>oc</sub> (mV)	J <sub>sc</sub> (mA/cm <sup>2</sup> )	FF (%)	η (%)
1	CW, 532 nm	2	633	37.4	78.9	18.7
1	ML, 355 nm	2	632	37.9	76.9	18.4
2	CW, 532 nm	8	636	36.9	79.1	18.4
2	ML, 532 nm	12	635	37.3	77.6	18.3

Overall, the best-cell performance parameters consist of efficiencies ranging from 18.3% to 18.7%, and fill factors from ~77% to ~79%. In both studies, LDSE processing with the Millennia 532-nm, 15-W CW laser was demonstrably superior, with a greater disparity when compared to the 355-nm vs. the 532-nm ML laser source.

## 5 ANALYSIS

### 5.1 Melt width of LDSE features

To determine initial laser parameters for LDSE processing, optical microscopy offers reasonably good information. When viewed under a microscope, the extent and strength of the laser-induced melting is clearly evident; and empirically, there is reasonably good correlation between the amount of laser melt and the strength of the corresponding doping.

For the 2<sup>nd</sup> study comparing 532-nm CW and ML lasers, initial optical microscope inspection of melt lines indicated that the ML laser could generate similar melt extent as the CW laser, but at higher scan speeds (Figure 5).

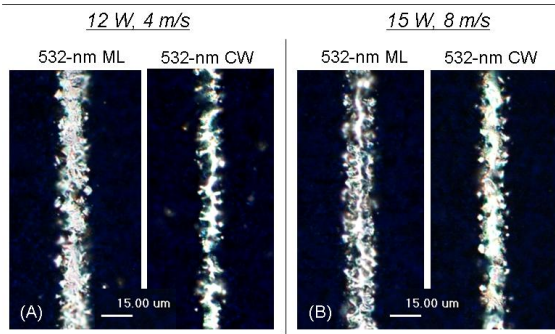


**Figure 5:** Microscope photos showing LDSE melt lines with 12-W, 4 m/s (A) and 15-W, 8 m/s (B) for 532-nm CW and ML laser sources.

The photos illustrate the stronger melt that occurred with the ML vs. the CW laser, in the form of (1) complete removal of the SiNx ARC layer, and (2) significant disruption of the alkali surface texturing. With both lasers, higher scan speeds and lower laser powers result in less disruption to the wafer texture. This indicates less severe melting and likely weaker and/or shallower doping.

### 5.2 Junction depth of LDSE features

While the melt width and strength at the wafer surface is fairly useful in ascertaining the strength of the laser doping, its value lies solely in the fact that it has

been empirically loosely correlated with the depth of the doped region that forms below the surface. To actually *measure* this doping/junction depth, the accepted reliable analytical technique is secondary ion mass spectrometry, or SIMS.

In the first study, comparing 355-nm ML and 532-nm CW lasers for LDSE processing, select features were treated with SIMS analysis. For the condition of 12-W power and 2-m/s scan speed, the concentration of the phosphorus dopant atoms was measured with increasing depth below the wafer surface. The collected data is displayed graphically in Figure 6.

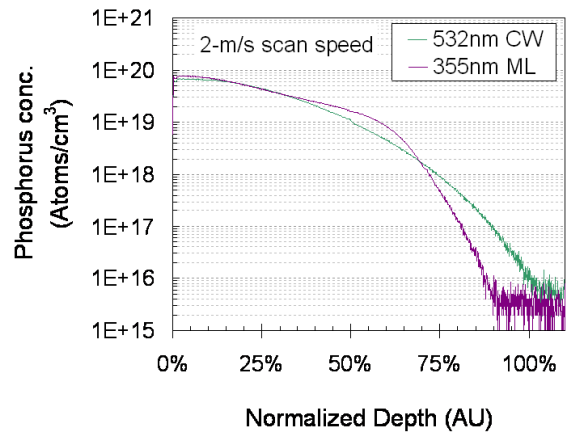


**Figure 6:** Phosphorous concentration with depth for lines scanned with 532-nm CW and 355-nm ML lasers at 12-W power at 2-m/s scan speed.

The SIMS analysis shows that for the same power and scan speed, the 532-nm CW laser generates deeper doping, resulting in a deeper junction. This is clearly evident in the data above for the 2-m/s scan speed; but it is not clear if this would necessarily hold true for other scan speeds.

While SIMS analysis yields the most accurate data for junction depth and dopant concentration analysis, it is expensive and time consuming, and not always readily available in areas lacking good analytical laboratory services. An alternative method for junction depth analysis that was explored is angle-lapping and junction staining. This process involves the following steps:

- Cleave the wafer in a direction perpendicular to the orientation of the laser-doped lines
- Angle-lap the exposed facet with a lapping block of known angle, thus elongating the length of the exposed facet by a known magnification factor
- Immerse the angle-lapped facet in a CuSO<sub>4</sub> solution and illuminate with bright light, resulting in copper plating of the laser-doped areas.
- Inspect and measure the features via optical microscopy

If the laser-processed lines are arranged on a sample in close proximity, several features can be analyzed on just a single angle-lapped sample. Such a case is demonstrated with the optical microscope photos in Figure 7, showing stained junctions for various process parameters of study 1.

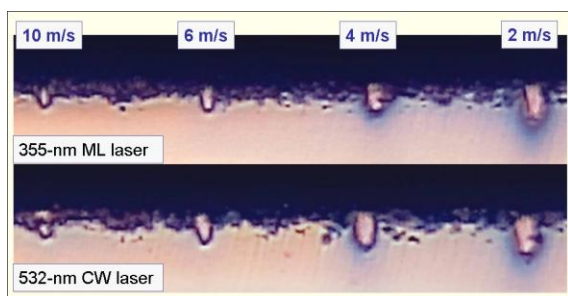


**Figure 7:** Cross-sectional view of angle-lapped and stained laser-doped features.

At a glance, the 532-nm CW features appear to be somewhat deeper, across all speeds, compared to the 355-nm ML features. This can be checked for by measuring the length of the features and plotting the data for each scan speed and for each laser system, as in Figure 8.

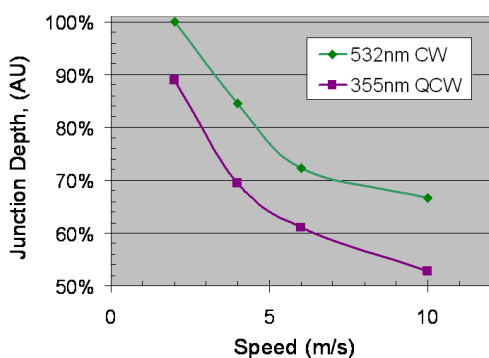


**Figure 8:** Normalized junction depth vs. scan speed as determined by measurement of angle-lapped and Cu-stained features for the 532-nm CW and 355-nm ML lasers.

The junction staining data shows the clear and continuous trend of deeper junction with the 532-nm CW laser. At the low 2 m/s scan speed, the data mirrors the SIMS data in Figure 6, with the ML laser junction depth 10% shallower than that formed with the CW laser. For increasing scan speeds, the discrepancy increases, with a ~20% shortcoming at the highest speed of 10 m/s. Clearly, for the same incident intensity, the 532-nm CW laser light is generating deeper doping profiles at higher scan speeds. The typical, actual range of junction depths generated via laser doping was around 1 – 3  $\mu\text{m}$ .

## 6 DISCUSSION & CONCLUSION

With various analysis techniques, combined with the cell performance data, a fairly clear picture of the LDSE processing performance has been created for the three lasers that were tested.

In the first study, there was a definite advantage demonstrated by the 532-nm continuous wave Millennia Prime laser. Using the same output power, beam focus size, and scan speeds (2, 6 m/s), consistently higher cell performance was achieved. This may be due to the difference in junction depths, with those generated by the 532-nm CW laser source being ~10 – 20% deeper. Since this depth disparity is on the order of several hundred nanometers; and considering that it is observed to

increase along with the scan speed, it can likely be explained by the greater optical absorption depth of the 532-nm light—which is about 1  $\mu\text{m}$  compared to ~10 nm for 355-nm).

In the second study, the 532-nm CW laser was found to produce slightly higher performing LDSE solar cells, albeit with slower scan speeds compared to the ML laser. While further optimization of the 532-nm ML process may result in improved LDSE cells (at the expense of scan speed, perhaps), it is not at all obvious if this is a likely—or even possible—outcome. In addition, any potential improvement over the CW laser process may be offset by considerations such as cost per watt and cost of ownership, both of which are historically higher for the ML laser technology.

LDSE is a promising process for high efficiency solar cells, and the choice of laser source can have a significant effect on cell performance. In various experiment studies, the 532-nm CW laser source has demonstrated good proficiency for meeting the demands of this technology.

## 7 REFERENCES

- [1] Carlsson, C., et. al., *Laser doping for selective silicon solar cell emitter*, Proceedings of 21st European Photovoltaic Solar Energy Conference, 2006; Dresden, Germany.
- [2] Kray, D., et. al., *Laser-doped silicon solar cells by laser chemical processing (LCP) exceeding 20% efficiency*, Proceedings of 33<sup>rd</sup> IEEE Photovoltaic Specialist Conference, 2008; San Diego, United States.
- [3] Ruby, D., et. al., *Recent progress on the self-aligned, selective-emitter silicon solar cell*, Proceedings of 26<sup>th</sup> IEEE Photovoltaic Specialists Conference, 1997; Anaheim, United States.
- [4] Tjahjono, B., et. al., *Optimizing Selective Emitter Technology in One Year of Full Scale Production*, Proceedings of 26th European Photovoltaic Solar Energy Conference, 2011; Hamburg, Germany.
- [5] Dubé, C., et. al., *High efficiency selective emitter cells using patterned ion implantation*, Proceedings of 1st International Conference on Silicon Photovoltaics, 2011; Freiburg, Germany.
- [6] S.R. Wenham and M.A. Green, *Self aligning method for forming a selective emitter and metallization in a solar cell*, Patent no. 6429037, 2002; United States.
- [7] Tjahjono, B., et. al., *High efficiency solar cell structures through the use of laser doping*, Proceedings of 22<sup>nd</sup> European Photovoltaic Solar Energy Conference, 2007; Milan, Italy.
- [8] Lawrence F. Durkee, *Method of plating by means of light*, Patent no. 4144139, 1979; United States.
- [9] Tjahjono, B., et. al., *18.9% efficient laser doped selective emitter solar cell on industrial grade p-type czochralski wafer*, Proceedings of 25th European Photovoltaic Solar Energy Conference, 2010; Valencia, Spain.
- [10] Sze, S. M., *Physics of Semiconductor Devices*, John Wiley and Sons, N.Y., 1981.
- [11] Sugianto, A., et. al., *18.5% laser-doped solar cell on Cz p-type silicon*, Proceedings of 35th IEEE Photovoltaic Specialists Conference, 2010; Honolulu, United States.